Annals of Nuclear Energy 198 (2024) 110291

Contents lists available at ScienceDirect

Annals of Nuclear Energy

journal homepage: www.elsevier.com/locate/anucene

# Deterministic neutron transport and burnup code coupling assessment

Arturo Vivancos [a], Rafael Miró [a,*], Teresa Barrachina [a], Álvaro Bernal [b], Gumersindo Verdú [a]

[a] Research Institute for Industrial, Radiophysical and Environmental Safety (ISIRYM), Universitat Politècnica de València (UPV), Camí de Vera, s/n, 46022 València, Spain

[b] Nuclear Safety Council. Calle Pedro Justo Dorado Dellmans, 11, 28040 Madrid, Spain

ARTICLE INFO

*Keywords:*
Depletion
Burnup
Neutron transport
Transition matrix
FVM
DO

ABSTRACT

Nuclide evolution is a key aspect in nuclear reactor design and operation. Burnup (or depletion) codes evaluate the isotopic inventory evolution. The inherent need for nuclear safety, the development in computational capabilities, and new discoveries in related areas, such as mathematical methods, result in constant software re-evaluation and improvement. Now, many stochastic-based burnup codes are being developed in comparison to deterministic-based ones, which also present advantages and interesting aspects. In this work, nuclear libraries, processing requirements, data workflow, and methodologies are studied for the development of a brand-new burnup code linked to the VALKIN-FVM-Sn deterministic transport code. As a result, the requirements to create, and couple, a burnup code have been assessed, establishing a methodology. The burnup code has been developed and contrasted with an industry reference. The resulting coupling is a lattice code foundation to be used in a Multiphysics platform.

## 1. Introduction

Nuclear fuel experiences a nuclide inventory evolution due to neutron-induced reactions and radioactive decay. Nuclide evolution is key in nuclear reactor design, operation, and safety analysis. The so-called burnup codes predict the isotopic inventory change by solving the equations modelling the phenomena.

Nuclide inventory evolution can be modelled as a first-order ODE system, whose solution has been widely studied (Cacuci, 2010). The most crucial factors regarding burnup simulations are the accuracy and uncertainty of the coefficients (reactions rates, decay constants and integral time-volume flux) defining the ODE system. Reactor physics codes with burnup capabilities can divided depending on the transport method used to generate the transition matrix: deterministic and probabilistic methods. On the one side, most of the recent developments make use of Monte Carlo based transport codes, such as ONIX (de Troullioud de Lanversin et al., 2021) and IMPC (Zhao et al., 2020) burnup codes, coupled with OpenMC (Romano et al., 2015), ALEPH-2 (Stankovskiy et al., 2012) and ACAB (Sanz et al., 2008) burnup codes, coupled with MCNP (Rising et al., 2023) or SERPENT (Leppänen et al., 2015), which embeds both transport and burnup codes. On the other side, a number of rector physics codes with depletion capabilities make use of deterministic solvers to perform the transport calculations namely, APOLLO3 (Schneider et al., 2016), WIMS-D (Lindley et al., 2017), or DRAGON (Marleau et al., 2016), all of which embed the transport and burnup solver. Some of the most used and deep-rooted codes in industry and research are transport based such as CASMO (Rhodes et al., 2006) or HELIOS-2 (Wemple et al., n.d.). In the case of the SCALE suite (Wieselquist et al., 2020), one can select whether to use a deterministic or stochastic based transport solver to be used for burnup calculations in the TRITON module. Independently of the transport solver used, ORIGEN burnup code performs the depletion calculations in SCALE.

This work is framed in the efforts of developing a lattice code to be used in a Multiphysics environment. The platform is intended to perform thermohydraulic and neutronic coupled calculations of nuclear components in 2D or 3D geometries. In this context, the present work aims to make use of an in-house advanced transport code, VALKIN-FVM-Sn (Bernal, 2018), to start the development of a new burnup code. This work's main objective is to create a new burnup code and to couple it to VALKIN-FVM-Sn, VALKIN from now on. VALKIN performs deterministic multigroup transport calculations using the Finite Volume Method (FVM) for spatial discretization, and the Discrete Ordinates (DO) method for the angular discretization; it will provide the target lattice code with 2D and 3D calculation capabilities using unstructured

* Corresponding author.
*E-mail addresses:* avivancos@upv.es (A. Vivancos), rmiro@upv.es (R. Miró), tbarrachina@iqn.upv.es (T. Barrachina), alvaro.bernal@csn.es (Á. Bernal), gverdu@iqn.upv.es (G. Verdú).

https://doi.org/10.1016/j.anucene.2023.110291
Received 30 June 2023; Received in revised form 29 November 2023; Accepted 6 December 2023
Available online 17 December 2023

arbitrary meshes. With this purpose, a burnup code was first developed in Matlab® (version R2022a) and coupled to VALKIN. The code implemented in Matlab® has proven to provide good results compared to industry reference programs (Vivancos et al., 2021). Once the Matlab® version was tested and verified, the burnup code was implemented in Fortran (GNU Fortran 8.5.0) and coupled to VALKIN. As a result, two depletion codes named DTCM and DTCF were developed in Matlab® and Fortran respectively and coupled to VALKIN. Nuclear data requirements, processing and methodology are studied to start the development of a brand-new burnup code. This paper starts with a brief introduction, in the second section, the theory framework is discussed, then, the third section introduces software and codes used in the work, in the fourth section, the code coupling and methodology developed are shared, then, results are presented in the fifth section, finally, conclusions and future work are presented in the sixth section.

## 2. Theory and procedures

As a new code is to be developed, an extensive study about current codes, trends, and methods was performed, focusing attention on data requirements and processing. It was determined to consider SCALE/ORIGEN (Gauld et al., 2011) as a standard reference because it is one the most notable and contrasted depletion software using a deterministic transport solver.

### 2.1. Burnup equations

The evolution of an isotope is evaluated as a balance between production and removal terms, resulting in first-order differential equation known as Bateman equation (Bateman, 1910). Bateman studied the evolution of nuclides contained in decay chains, forming coupled sets of Bateman equations. For simple problems and conditions, an analytical solution was proposed. The Bateman equation was extended to include terms arising from neutron-induced reactions. The general Bateman equation, depicting a nuclide concentration evolution during time is presented as in Eq. (1):

$$\frac{dN_i}{dt} = \sum_{j(j\neq i)} (b_{i,j}\lambda_j + \sum_k \gamma_{i,j,k}\sigma_{j,k}\phi)N_j - (\lambda_i + \sigma_{rem,i}\phi)N_i \quad (1)$$

where.

- $N_i$ is the atom density of nuclide $i$
- $b_{i,j}$ is the branching ratio from nuclide $j$ to $i$
- $\lambda_j$ is the decay constant of nuclide $j$
- $\phi$ is the space- and energy-averaged neutron flux
- $\sigma_{j,k}$ is the microscopic cross section of reaction $k$ for nuclide $j$
- $\sigma_{rem,i} = \sum_k \sigma_{i,k}$ is the removal cross section of nuclide $i$, obtained by adding all possible neutron-induced reactions $k$ that nuclide $i$ can experience
- $\gamma_{j,i,k}$ is the production yield of nuclide $i$ due to the reaction $k$ occurred in nuclide $j$, including the non-fission and fission events

Depending on the existence, lack or predominance of certain transmutation mechanisms, nuclides are organized into three groups (Marguet, 2017): heavy nuclides or actinides, fission products, and activation products or light nuclides. Eq. (1) can be rearranged and presented in many forms. It is interesting to group together the flux-dependent terms as follows, Eq (2):

$$\frac{dN_i}{dt} = (\sum_{j(j\neq i)}\sum_k (\gamma_{i,j,k}\sigma_{j,k})N_j - \sigma_{rem,i}N_i)\phi + \sum_{j(j\neq i)} (b_{i,j}\lambda_j)N_j - \lambda_i N_i \quad (2)$$

The former step is done to separate the problem-independent (decay constants and decay branching ratios) from the problem-dependent parameters (flux, cross sections, and fission yields). Note that, on the right-hand side, the two summations in the flux-dependent term could seem to be reiterative. However, it is necessary to consider both summations, one for nuclides, and one for reactions; a nuclide $j$ could contribute to a nuclide $i$ by means of two neutron-induced reactions e.g., $(n, n^3He)$ and $(n, \alpha)$.

Burnup calculations are always performed for one-group energy structure. All energy-dependent parameters must be collapsed (flux and cross sections) or interpolated (fission yields) to a single group.

### 2.2. Burnup ODE system

The isotopic evolution of a material exposed to a neutron flux, and experiencing radioactive decay, is defined by a set of coupled Bateman equations. This leads to a set of coupled first order differential equation system, ODE system. For simple problems, it is possible to find an analytical solution to the problem, however in burnup calculations it is necessary to rely on numerical methods.

Bateman equations coefficients vary with time as flux and cross sections depend on the changing nuclide inventory. However, the coefficients are considered to be constant for intervals of time denoted as depletion steps. A long period of interest, for instance, a complete nuclear fuel cycle, is split into several depletion steps. Even though, it implies a source of error, this error can be minimized by two techniques, the predictor–corrector and the sub-step method, explained on (Cacuci, 2010) and (Wieselquist et al., 2020).

The ODE equation system is written in matrix form for a depletion step $n$, as in Eq. (3):

$$\frac{d\vec{N}}{dt} = A\vec{N}(t) = (A_{\sigma,n}\phi_n + A_\lambda)\vec{N}(t) \quad (3)$$

where

- $A$ is the so-called "transition matrix" which holds the ODE coefficients (nuclide transition ratios)
- $\vec{N}(t)$ is the concentration vector
- $A_{\sigma,n}$ is the "neutron transition matrix", which contains the neutron induced rates for step $n$
- $\phi_n$ is the space- and energy-averaged neutron flux for step $n$
- $A_\lambda$ is the "decay transition matrix"

The last system is a very well-known problem appearing in many fields and widely studied (Moler and Van Loan, 2003), (Cetnar, 2006), (Josey et al., 2017), and (Pusa, 2013). The transition matrix is always a square sparse matrix.

In the burnup case, the system is extremely stiff as the transmutation rates (matrix coefficients) can vary from low to great values (both cases due to decay coefficients), what leads to huge matrix norms (Pusa, 2013). In the cases studied for this work, transmutations rates had order of magnitudes between $10^{-33}$ and $10^2$, with norms over $10^3$. Fig. 1 shows a representation of the transition matrix $A$ for 1327 nuclides (square matrix of dimension 1327). The 176 first nuclides are actinides, and the rest, fission products. The sparsity of the matrix is evident in the representation, it can also be seen that fission products can appear from actinide's fission reaction (rectangular block on left side). All diagonal elements are negative values accounting for each nuclide loss ratio.

### 2.3. Burnup chains

Nuclear fuel under operation contains thousands of nuclides. While it is subject to a neutron flux, nuclides can experience several dozens of transitions caused by neutron-induced reactions and decay processes. This leads to big transition matrices. In conventional light water reactors, core dynamics and performance are mostly affected by a reduced number of nuclear species, neutron reactions, and decay processes. It is possible to determine a shortened number of nuclides and transitions to adequately study a system's performance (Oka et al., 2014). These sets

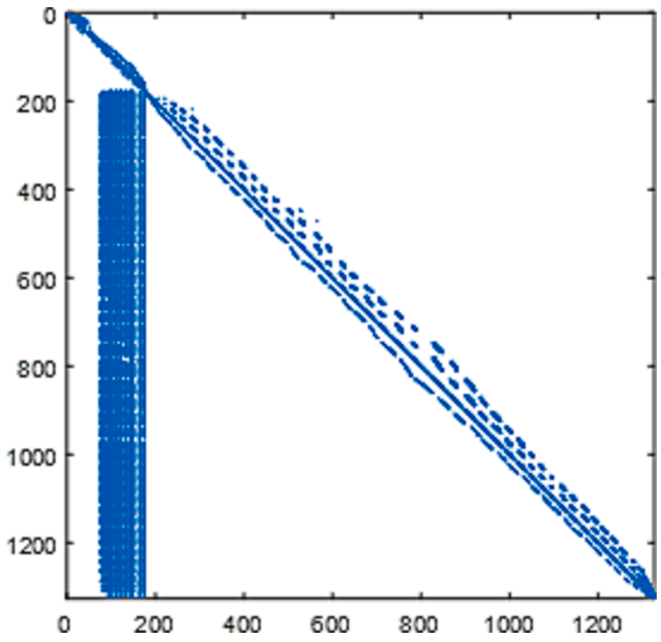


**Fig. 1.** Burnup matrix representation for 1327 nuclides.

of contracted nuclides and transitions are known as reduced burnup chains. Traditionally, reduced burnup chains have been, and are, used to study the system's design and performance, (IAEA, 2007), (Okumura et al., 2007), and (Aldama, 2014). Nowadays, computation capabilities allow to consider thousands of nuclides with many neutronic-induced and decay transitions. SCALE's fission products and actinides burnup chain has been used in this workTable1.

At the current code under development status, only actinides (or heavy nuclides) and fission products are being considered, excluding light nuclides (or activation products). SCALE uses 1327 nuclides between actinides (176 nuclides) and fission products (1151 nuclides). For transmutation mechanisms, 21 neutron-induced reactions and 11 decay transitions are used, as shown in and Table 2 ([*m*0] and [*m*1] indicates whether the decay is to ground or first excited state, *m* is used for de-excitation, and *n* for neutron emission).

**Table 1**
Neutron reactions processes considered.

| Neutron-induced reactions Number | MT number | Reaction |
|---|---|---|
| **1** | 16 | (n, 2n) |
| **2** | 17 | (n, 3n) |
| **3** | 18 | (n, fission) |
| **4** | 22 | (n, nα) |
| **5** | 24 | (n, 2nα) |
| **6** | 28 | (n, np) |
| **7** | 29 | (n, n2α) |
| **8** | 32 | (n, nd) |
| **9** | 33 | (n, nt) |
| **10** | 34 | (n, $n^3$He) |
| **11** | 37 | (n, 4n) |
| **12** | 41 | (n, 2np) |
| **13** | 102 | (n, γ) |
| **14** | 103 | (n, p) |
| **15** | 104 | (n, d) |
| **16** | 105 | (n, $^3$He) |
| **17** | 106 | (n, t) |
| **18** | 107 | (n, α) |
| **19** | 108 | (n, 2α) |
| **20** | 111 | (n, 2p) |
| **21** | 112 | (n, pα) |

**Table 2**
Decay processes considered.

| Decay mechanisms Number | Decay |
|---|---|
| **1** | $\beta^-$[m0] |
| **2** | $\beta^-$[m0] + α |
| **3** | $\beta^-$[m1] |
| **4** | $\beta^-$[m0] |
| **5** | $\beta^-$[m0] + α |
| **6** | $\beta^-$[m0] + n |
| **7** | $\beta^+$[m0] |
| **8** | $\beta^+$[m1] |
| **9** | α [m0] |
| **10** | α [m1] |
| **11** | m |

### 2.4. Problem-dependent data and burnup data libraries

Transport and burnup codes are used in tandem to evaluate the nuclide inventory evolution. For each depletion step, given the composition at the beginning of the step, the transport code generates the neutron flux in each material to be depleted. The neutron flux is then used to obtain the problem-dependent data characterizing Equation (1). With the transition matrix fully formed, the burnup code evaluates the nuclide evolution during the step and provides the concentration at the end. These concentrations will be the parting point for the next step's transport calculation.

The problem-dependent parameters, cross sections, fission yields, and integral flux, are calculated with a combination of problem-independent depletion libraries, problem-dependent cross sections, and the neutron flux generated by the transport code, $\phi_m^g$. The depletion libraries hold pre-processed cross sections, fission yields, and energy released information. In this work, SCALE/ORIGEN data libraries are used. Departing from the original libraries, new libraries were created, re-arranged, and indexed. Next, a brief description of the libraries is provided:

- **Depletion Neutron library**. Holds information for 774 targets nuclides and is based on the JEFF-3.0/A (NEA, 2005). The 56-group neutron resource is used. Neutron resource library is pre-processed and collapsed using a thermal Maxwellian-1/E-fission-1/E weighting spectrum. The Depletion Neutron Library will be referred to as DNL from now on. For some nuclides and cross sections, self-shielding effect must be considered to appropriately estimate the transmutation ratios. For this reason, a set of nuclides' cross sections must be updated in DNL with problem-dependent processed cross sections.
- **Decay library.** Decay data is based on the ENDF/B-VII.I (Chadwick et al., 2011).
- **Fission yields library.** Independent (direct) fission yields are considered for 30 fissionable actinides and tabulated for 3 energies, thermal, fast, and high energy. Except from few exceptions to address inconsistencies, they come from the ENDF/B-VII.0 (Chadwick et al., 2006).
- **Energy released library.** Energy released by both capture and fission are needed to compute the space- and energy-averaged neutron flux ($\phi_n$). These values are mainly from ENDF/B evaluations. Most nuclides are assumed to have a fission recoverable energy of 200 MeV and 5.0 MeV, with the exception of listed on SCALE/ORIGEN manual (Wieselquist et al., 2020).

The processing procedure followed by the burnup codes developed, DTCM and DTCF, is analogous to the one depicted and used in SCALE/ORIGEN (Wieselquist et al., 2020). Nuclide cross sections $\sigma_{j,k}$ are collapsed to one group (**Error! Reference source not found.Error! Reference source not found.**), removal cross section (Eq. (5), and the

average fission energy at which fissions take place for each fissionable nuclide, (Eq. (6) are computed**Error! Reference source not found.**:

$$\sigma_{j,k} = \frac{\sum_g \sigma^g_{j,k} \phi^g_m}{\sum_g \phi^g_m} \tag{4}$$

$\sigma^g_{j,k}$ is the group $g$, reaction $k$ cross section for nuclide $j$, from the neutron library.

$$\sigma_{j,rem} = \sum_k \sigma_{j,k} \tag{5}$$

$$\overline{E}_{j,f} = \frac{\sum_g \overline{E}^g \sigma^g_{j,f} \phi^g}{\sum_g \sigma^g_{j,f} \phi^g} \tag{6}$$

$\overline{E}^g$ is the average energy in the group $g$, corresponds to midpoint energy within each group's boundaries, $\sigma^g_{j,f}$ is the fission cross section for nuclide $j$ and group $g$.

Fission yield $\gamma_{j,i,k}$ is interpolated using the average fission energy from (Eq. (6), $\overline{E}_{jf}$.

Space- and energy-average neutron flux is computed (Eq. (7).

$$\phi = \frac{P}{\sum_j (\kappa_{jf}\sigma_{if} + \kappa_{jc}\sigma_{jc}) N_j(t)} \tag{7}$$

$P$ is the average specific power in the material (MW/MTU), $\sigma_{jc}$ is *capture* cross section defined as removal minus fission, $\kappa_{jf}$ and $\kappa_{jc}$ are nuclide $j$ energy released per fission and *capture* from the energy released library, and $N_j(t)$ is nuclide $j$ concentration.

## 3. Software and codes

Cross section processing and transport calculations are very sensitive and important aspects in nuclear physics codes. There are two main approaches to solve the transport problem in nuclear physics: deterministic and stochastic (Monte Carlo). Whereas Monte Carlo transport solvers are able to work with both continuous-energy and multigroup data, deterministic solvers have to draw on multigroup theory and procedures, resulting in the need for self-shielding treatment and correction before transport calculations.

In the following sections, software used in the work is described.

### 3.1. Scale

The SCALE suite is used as a reference to evaluate the coupling under development. For depletion calculations, SCALE counts with a control module called TRITON (DeHart et al., 2003), which couples and communicates several modules to perform depletion calculations for a wide range of conditions and methods. To perform depletion calculations, cross section processing (if required), transport calculations, and inventory evolution calculations are to be performed for each depletion step.

TRITON can perform depletion calculations based on deterministic or stochastic transport approaches. On the one hand, the modules XSDRNPM (1D) and NEWT (2D) (DeHart, 2006) can be used for deterministic calculations. On the other hand, KENO-V.a and KENO VI modules can be used for 3D Monte Carlo transport calculations. Whereas Monte Carlo based transport modules can either perform continuous energy or multigroup calculations, the deterministic modules always make use of the multigroup approach. For KENO-V.a and KENO VI using multigroup data, and always in the case of the deterministic solvers, cross section processing is to be performed prior to transport calculations. For cross section processing, TRITON uses XSProc module, that generates problem-dependent multigroup self-shielded cross sections. Finally, ORIGEN is the module in charge of evaluation the isotopic inventory evolution once the transport calculation is finished.

In this work SCALE depletion calculations are performed using the deterministic transport code NEWT, and thus, XSProc for cross section processing. The control sequence followed by TRION for each depletion step is: XSProc, NEWT, and finally ORIGEN. Further information about the modules and parameters used for the calculations can be found next:

- **XSProc** is the cross-section processing module. XSProc generates temperature corrected and self-shielded microscopic cross sections for each material in the model. The default option for cross section processing is used. First, self-shielded cross sections are generated by the Bondarenko method using infinite-dilute self-shielded cross sections with a generic weighting spectrum. Secondly, point-wise transport calculations are performed at pin level to obtain the problem-dependent material flux spectrum. Finally, the point-wise flux spectrum is used to generate new self-shielded cross sections. In this work, SCALE's 56-energy group ENDF/B-VII.I transport cross section library is used.
- **NEWT** is the code used for transport calculations in this work. NEWT is a 2D deterministic discrete-ordinates transport code. It uses multigroup cross sections generated by XSProc. It works with the Extended Step Characteristic approach for the spatial discretization and the discrete-ordinates method for the angular discretization. For this work a level symmetric quadrature set of 6 (Sn = 6) is used.
- **ORIGEN** is the module in charge of evaluating materials isotopic evolution. For depletion calculations all energy parameters are collapsed or interpolated to one energy group. TRITON departs from the material flux spectrum generated by the transport code and provides ORIGEN with the step dependent data that characterize the isotopic evolution. ORIGEN uses a predictor–corrector approach, it predicts the nuclide inventory at the mid-point of each depletion sub-interval. Then, cross section and transport calculations are performed at the mid-point to generate the reactions rates used to perform the depletion for the whole sub-interval. Two methods are available in ORIGEN for solving the depletion ODE system: MATREX and CRAM. MATREX is a tailor-made solver kernel with two different approaches for short- and long-lived nuclides. The Chebyshev Rational Approximation Method (CRAM) (Leppänen et al., 2015; Pusa, 2013) is a matrix exponential method recently developed and widely spread for burnup calculations. In this work MATREX is used as it is SCALE's default option.

### 3.2. Valkin-fvm-sn transport code

Burnup codes must be fed with a transition matrix to evaluate the nuclide evolution for a depletion step. The transition matrix coefficients vary with time as it is partly formed by parameters that depend on the neutron spectrum and distribution (cross sections, fission yields, branching ratios, and integral flux). These coefficients are problem-dependent and must be generated for each depletion step with information provided by a transport code. Transport codes can be classified into deterministic and stochastic, both of which have strengths and weaknesses (Wieselquist et al., 2020), (Josey et al., 2017), (Wagner et al., 2011), and (Haeck et al., 2017). One of the main deterministic code's drawbacks, is their general limitation to deal with complex geometries.

VALKIN is an advanced 3D time-dependent multigroup neutron modal code based on the Discrete-Ordinates method for angular discretization and the Finite Volume Method for the spatial discretization, it considers upscattering and downscattering with any number of energy groups, and can be used with different quadrature options. The FVM method applied to solve the Boltzmann equation has been studied recently (Bernal, 2018), (Hu et al., 2017), and (Wang et al., 2017). It is based on the SLEPc eigenvalue calculation library (Hernández et al., 2005). VALKIN has proven to provide good flux distribution spectra, and multiplication factor results for complete fuel assemblies as seen in (Labarile et al., 2021) and (Barrachina et al., 2022). The use of the FVM

method allows VALKIN to overcome one the main inconveniences of many transport solvers, the use of 2D cartesian meshes. VALKIN can perform neutron transport calculations using unstructured meshes for arbitrary geometries, providing the capability of modelling complex geometries with high level of detail. It also has the potential to perform 3D nodal transport calculations. 2D/3D geometry and mesh input deck for VALKIN can be processed with the open source ***Gmsh*** mesh generator code (Geuzaine and Remacle, 2009), while the results are obtained in ASCII and.*vtk* formats.

The burnup code under development joint with VALKIN, and a cross section processing code, also under study, will conform the lattice code used in a Multiphysics platform. The main goal of creating a burnup code from the ground up is the advantage of having full control and knowledge of it. This results in a more flexible code, facilitating future developments and enhancements. It will ease future tests and approaches to the burnup problem in the Multiphysics platform, as the study of detailed local burnup effects in critical locations or components.

Conversely, to stochastic codes, able to work with continuous-energy cross sections, deterministic codes use the multigroup approach. When using a deterministic transport code, a cross section processing is to be performed prior to the transport calculations. The processing is performed to consider temperature, space, and self-shielding effects on the cross sections. For this work, the SCALE's module XSProc is used to generate the problem-dependent cross sections to be used by VALKIN. SCALE's 56-group cross section library based on the ENDF/B-VII.I (Chadwick et al., 2011) is used in XSProc to generate the problem-dependent cross sections for transport calculations in VALKIN. In regards of the discrete ordinate's method, the calculations are

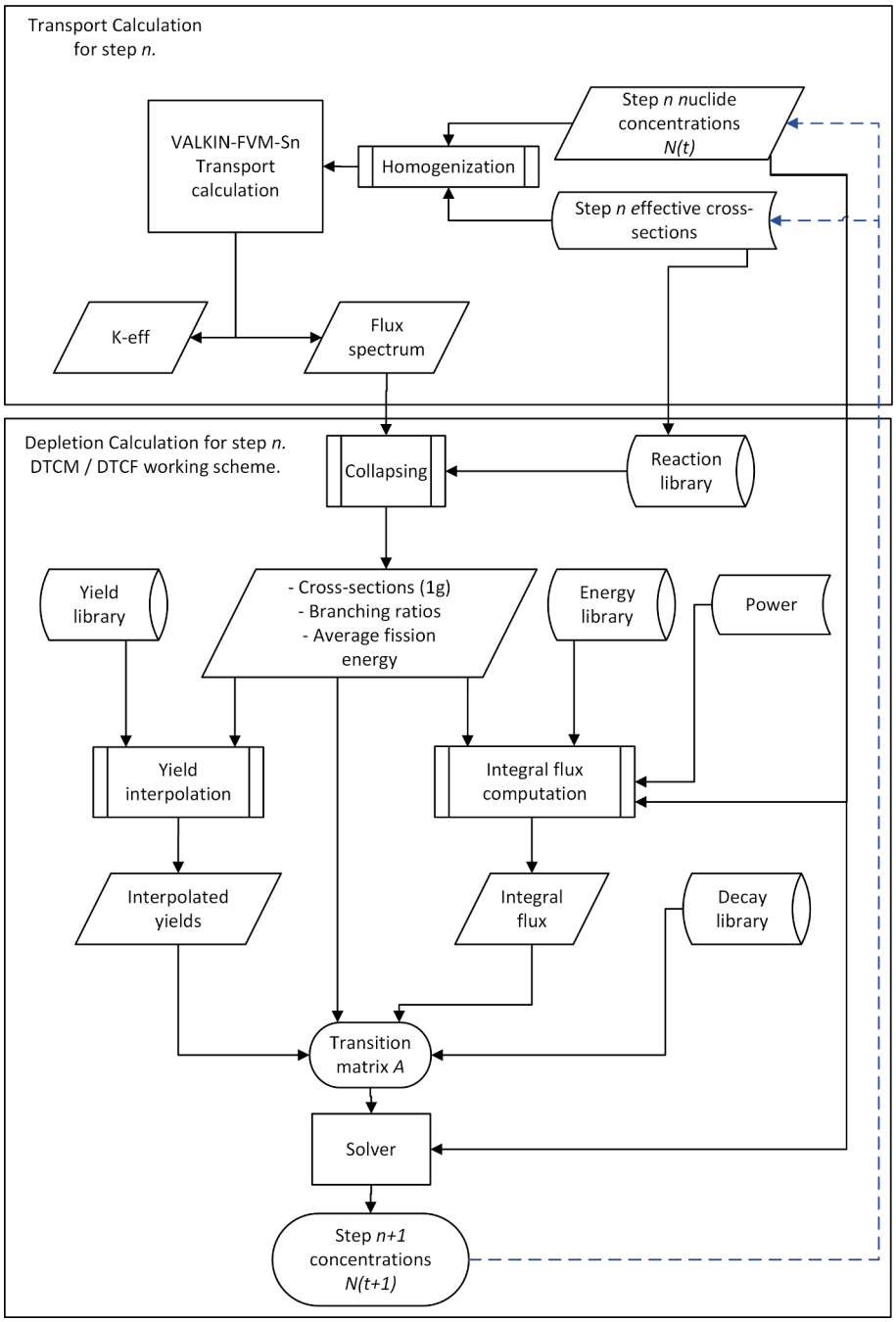


**Fig. 2.** Data processing flow chart for each depletion step.

performed with an order 6 Level Symmetric quadrature.

### 3.3. ODE system solvers

In the present work, *ode15s* solver (Shampine and Reichelt, 1997) was used in Matlab® implementation, and *lsode* in Fortran implementation. Although *ode15s* is not as sophisticated and advanced as the solvers used in other programs, it has proven capable of providing good results in comparison to reference codes such as SCALE/ORIGEN, (Vivancos et al., 2021). Matlab® has played a key role in the development and coupling of the Fortran code. Some tests are also easier to perform in Matlab®, furthermore, it is more suitable for academic purposes. For these reasons, the Matlab® code was developed and will be maintained.

In the case of *lsode*, it is part of ODEPACK (Hindmarsh, 1983), which is used in depletion codes as FISPACT-II (Sublet et al., 2017).

Both, *ode15s* and *lsode* are suitable for solving stiff systems and make use of the Backward Differentiation Formula method for stiff problems.

## 4. Code coupling and data processing

As a burnup code is being developed from the ground up, many tasks and verifications are being evolved in parallel. Prior to this work, it was verified that both, Matlab® (using *ode15s*) and Fortran (using *lsode* (Radhakrishnan and Hindmarsh, 1993)) could perform burnup calculations using SCALE's transition matrices with satisfactory results. Now, the focus is on generating transition matrices parting from neutron flux spectra computed with VALKIN and the data libraries obtained from SCALE. One of the tasks currently under development is the development of a problem-dependent self-shielded cross sections module. At this moment, effective cross sections are generated using SCALE's XSProc sequence for each depletion step and transport calculation.

In Fig. 2, the working flow and data transfer followed between the transport and depletion calculations is depicted, this process is followed for each depletion step and material to be depleted. The flowchart is divided in two different blocks. The first one refers to the transport sequence. The second one corresponds to the depletion calculations, describing the codes developed, DTCM and DTCF.

In the first block, for a given isotopic inventory, nuclide's problem-dependent microscopic cross sections are generated using SCALE for each depletion step. Self-shielded cross sections were translated to ASCII format using the PALEALE tool from AMPX-6 system (Wiarda et al., 2016). With problem-dependent microscopic cross sections and nuclide's concentrations for each material, homogenization processing is to be performed to obtain material macroscopic cross sections. The macroscopic cross sections are then used in VALKIN's transport calculation. VALKIN provides the neutron flux spectrum for all cells in the model mesh, with which material integral flux spectrum is obtained, $\phi_m^g$.

In the second block, and after the transport calculation, DTCM and DTCF are fed with material flux spectrum, nuclide concentrations, and self-shielded cross sections (the same used in the transport calculations and generated with SCALE). At this point, procedure depicted in item 2.4 is followed and the depletion calculations is performed, generating the new isotopic inventory at the end of the step. If further steps are to be performed the process is restarted with the new inventory.

## 5. Results and discussion

To verify libraries generated and data processing implemented in DTCM and DTCF, depletion calculations were performed and evaluated comparing with TRITON, using the transport module NEWT. For transport calculations, NEWT and VALKIN are used with an order 6 Level Symmetric quadrature for the Discrete Ordinates method, and reflective boundary conditions. The 56 groups SCALE's cross section library is used to compute the reference results and to generate the self-shielded cross sections to be used in VALKIN.

The model used to verify the code is a PWR fuel rod. It corresponds to the TMI-1 PWR unit cell from the UAM benchmark (Ivanov et al., 2013). Model information can be found in Table 3 and Fig. 3. Once the DTCM implementation is verified it will be implemented and evaluated in Fortran, DTCF.

Burnup calculations are performed for 365 days with 25 MW/MTU constant power density, the final burnup is 9.125 GWd/MTU. In Fig. 4 the unstructured mesh used in VALKIN calculations is shown. The mesh was created with ***Gmsh*** (Geuzaine and Remacle, 2009). Only the nuclear fuel results are evaluated in this work.

Relative errors were computed as in Eq. (8), considering SCALE results as reference.

$$Rel.Error(\%) = \frac{SCALEvalue - value}{SCALEvalue} 100 \tag{8}$$

### 5.1. VALKIN transport calculation

For each depletion step, nuclide's microscopic cross sections generated by XSProc are homogenized to material level using current-step nuclide concentrations. Then, VALKIN is fed with problem dependent material cross sections.

In order to verify that cross sections are correctly homogenized, transport parameters are adequate, and fuel rod is correctly modelled, the effective multiplication factor and flux spectrum are compared for zero burnup.

In Table 4, it is appreciated that the error between SCALE's and VAKLIN's effective multiplication factor is over 75 pcm, what is considered an acceptable deviation.

Transport calculation is performed to obtain material flux spectra, $\phi_m^g$, for each depletion step. Normalization is needed for flux comparison, satisfying Eq. (9) condition. Fuel's normalized flux spectra for burnup 0 is shown in Fig. 5 for both SCALE and VALKIN.

$$\sum_g \phi_m^g = 1 \tag{9}$$

Fluxes result in an excellent match, and thus, transport calculation and procedures are considered validated.

### 5.2. Cross sections collapsing and transition matrix generation

Once transport calculation is performed, VALKIN provides material flux spectrum to perform cross section collapsing, which is the first step to generate transition matrix coefficients. With available flux spectra and the Depletion Neutron Library (DNL), collapsing is an unequivocal procedure. In this work, default DNL was initially used to generate the transition matrix. Then, DNL was updated with self-shielded cross

**Table 3**
Model data and specifications.

| Parameters | Value |
|---|---|
| Unit cell pitch, [mm] | 14.427 |
| Fuel pellet diameter, [mm] | 9.391 |
| Fuel pellet material | $UO_2$ |
| Fuel density, [g/cm$^3$] | 10.283 |
| Fuel enrichment, w/o | 4.85 |
| Cladding outside diameter, [mm] | 10.928 |
| Cladding thickness, [mm] | 0.673 |
| Cladding material | Zircaloy – 4 |
| Cladding density, [g/cm$^3$] | 6.55 |
| Gap material | He |
| Moderator material | $H_2O$ |
| Fuel temperature, [K] | 900 |
| Cladding temperature, [K] | 600 |
| Moderator (coolant) temperature, [K] | 562 |
| Moderator (coolant) density, [kg/m$^3$] | 748.4 |
| Power density, [MW/MTU] | 25 |

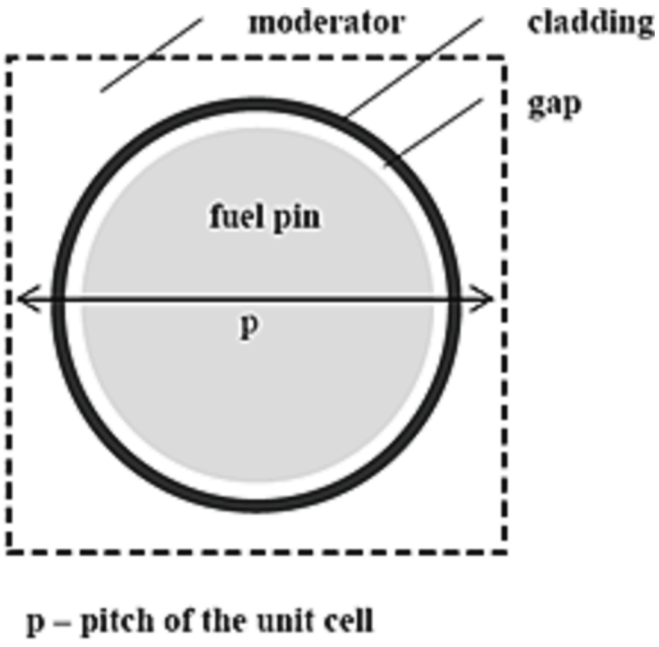


**Fig. 3.** Fuel rod.

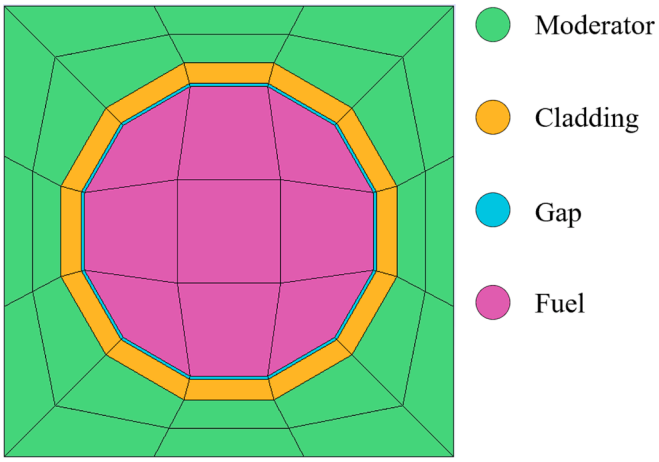


**Fig. 4.** VALKIN-FVM-Sn model mesh.

**Table 4**
Multiplication factor for 0 burnup.

| | SCALE | VALKIN | Error (pcm) |
|---|---|---|---|
| $k_{eff}$ | 1.40427 | 1.40352 | 75 |

sections. One-group cross sections generated with default and updated DNL were compared to evaluate the impact of self-shielding effects on burnup calculations.

In the first place, DNL default cross sections were collapsed using VALKIN's flux, resulting one-group cross sections were compared to SCALE's transition matrix values. For certain nuclides, collapsed cross sections from the DNL differed considerably from SCALE's. It was the case for nuclides listed in Table 5, which are very sensitive to self-shielding effects.

Thus, for each depletion step to be performed, DNL cross sections for nuclides in Table 5 must be substituted for self-shielded cross sections to account for local and case-specific resonant effects. After updating DNL with self-shielded cross sections, collapsed cross sections matched well with SCALE's transition matrix. In Table 6, Table 7, Table 8, and Table 9, collapsed values for relevant cross sections and nuclides are shared and compared. SCALE's transition matrix cross sections are listed in the first data column. The second column contains collapsed cross sections from the default DNL, the third column holds collapsed self-shielded cross sections used for transport calculations, denoted as SSXS. Note that in this work, self-shielded cross sections have been generated using SCALE's **XSProc** module prior to the transport calculation. Both DNL and SSXS cross sections are collapsed using the flux spectrum provided by VALKIN. Finally, the fourth and fifth columns hold relative differences between SCALE and DNL, and SSXS, respectively. In the case of U-235, DNL collapsed cross sections do not differ much in comparison to SCALE. However, for the rest of nuclides, the difference is very high. Some of the DNL collapsed cross sections reach relative differences over 100 % in absolute value, as in the case of Ru-103 radiative capture $(n,\gamma)$, which presents an error over −288 %. Nevertheless, once they are substituted with SSXS collapsed cross sections, most errors are below 1 %.

With proper collapsed cross sections, integral flux and interpolated yields are obtained, and all step dependent data is available to form the transition matrix.

### 5.3. Burnup results

After evaluating the transport calculation and cross section processing at 0 burnup, the system response is studied during burnup. The main parameters used to evaluate the code are nuclides concentrations and $k_{eff}$ evolution. The irradiation cycle is divided into 16 uniformly distributed depletion steps, for which the multiplication factor and nuclide concentration evolution are studied. Each depletion step has a time length of 22.8125 days, and the fuel is depleted with a specific power of 25 MW/MTU per day, resulting in 0.57 GWd/MTU accumulated burnup for depletion step. In addition, cross section collapsing is also evaluated for the 8th and 16th depletion step. For the cross sections evaluation during the burnup, only corrected collapsed cross section will be shared.

Table 10, Table 11, Table 12, and Table 13 SSXS collapsed cross sections are shown for the 8th and 16th depletion step. In all cases, the error for $(n, 2n)$ reaction increases with the burnup, reaching over a 3 % at the 16th depletion step. All cross sections' errors for Gd-155 augment with the depletion, for U-238 and Ru-103, the error is similar for the whole depletion for all reactions but $(n, 2n)$. In the case of U-235, the errors at 8th are below 1 % in absolute value but they increase at the 16th depletion step.

Some of the cross sections reached absolute relative errors over 3 %. Although some errors in the cross sections increase as the burnup does, these deviations are considered bearable as the main parameters of interest, concentrations and $k_{eff}$, present a good response and match with the reference values during the whole depletion. In Table 14, the concentrations for relevant nuclides (She et al., 2013; Zhang et al., 2020; Zhao et al., 2020) in atoms per barn·centimeter are shared, the error between the coupling values and the references are mostly below 1 % in absolute value.

Good results are obtained for $k_{eff}$ during the irradiation time. The $k_{eff}$ evolution for both SCALE and VALKIN is considerably similar in tendency and values, Fig. 6 presents its evolution along all depletion steps, the difference in *pcm* is maintained practically constant during the whole depletion. In addition, nuclide concentrations at the end of the depletion show a good agreement between both SCALE and the developed code. Finally, Fig. 7, Fig. 8, Fig. 9, and Fig. 10 share relevant nuclides evolution, the inventory agreement between codes is kept during the whole depletion, their evolution is considerably similar. In the case of Xe-135 and Cs-137 the error during the depletion is relatively constant, whereas for U-235 and Pu-239 it increases over the depletion. The increase in the error for the actinides could be caused by the corrector-predictor approach used by SCALE, but not implemented in the

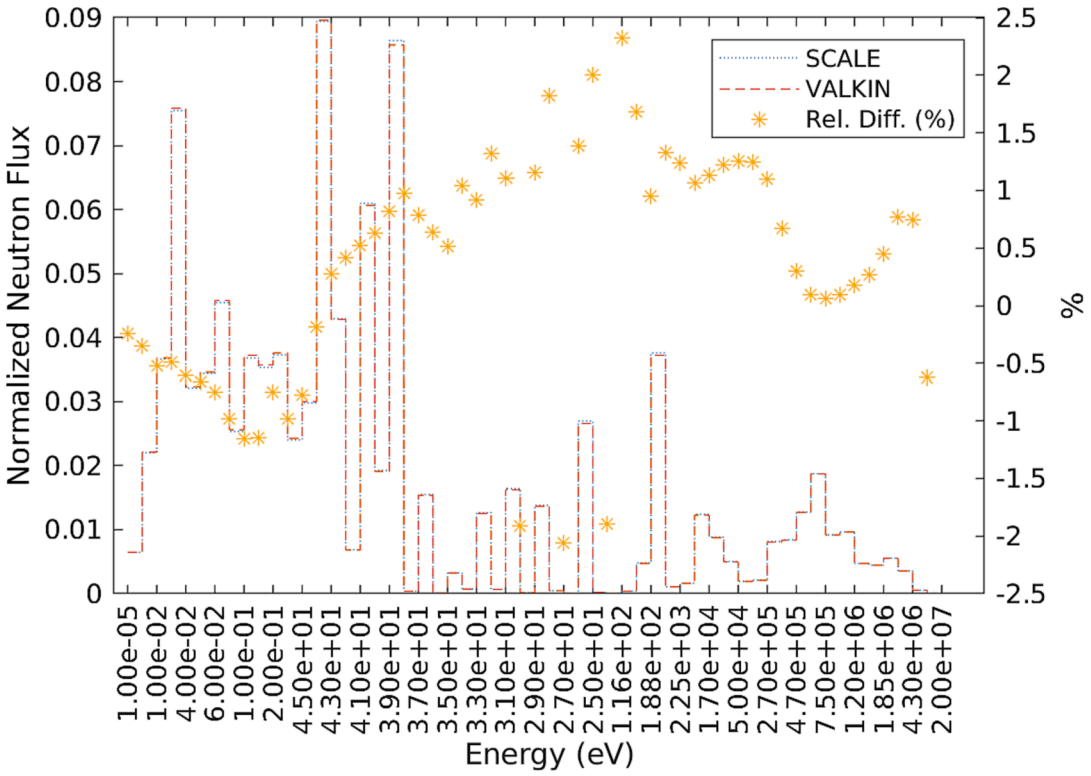


**Fig. 5.** SCALE/VALKIN normalized flux for 0 burnup.

**Table 5**
Self-shielding sensitive nuclides.

| | | | | | | | | | |
|---|---|---|---|---|---|---|---|---|---|
| H-1 | B-10 | B-11 | N-7 | O-16 | O-17 | O-18 | Kr-83 | Zr-91 | Zr-93 |
| Zr-94 | Zr-95 | Zr-96 | Nb-93 | Nb-95 | Mo-95 | Mo-97 | Mo-98 | Mo-99 | Mo-100 |
| Tc-99 | Ru-101 | Ru-102 | Ru-103 | Ru-104 | Ru-106 | Rh-103 | Rh-105 | Pd-106 | Pd-107 |
| Pd-108 | Ag-109 | In-113 | Xe-131 | Xe-133 | Xe-135 | Cs-133 | Cs-134 | Cs-135 | Cs-137 |
| Ba-140 | La-139 | Ce-141 | Ce-142 | Ce-143 | Ce-144 | Pr-141 | Pr-143 | Nd-143 | Nd-144 |
| Nd-145 | Nd-146 | Nd-147 | Nd-148 | Pm-147 | Pm-148 | Pm-149 | Sm-147 | Sm-149 | Sm-150 |
| Sm-151 | Sm-152 | Sm-153 | Eu-151 | Eu-153 | Eu-154 | Eu-155 | Eu-156 | Gd-152 | Gd-154 |
| Gd-155 | Gd-156 | Gd-157 | Gd-158 | Gd-160 | U-234 | U-235 | U-236 | U238 | Np-237 |
| Pu-238 | Pu-239 | Pu-240 | Pu-241 | Pu-242 | Am-241 | Am-242 | Am-243 | Cm-242 | Cm-243 |
| Cm-244 | Cm-242 *m* | | | | | | | | |

**Table 6**
Collapsed cross section comparison for U-235.

| **U-235 Cross section** | **SCALE (barn)** | **DNL (barn)** | **SSXS (barn)** | **SCALE/DNL relative difference (%)** | **SCALE/SSXS relative difference (%)** |
|---|---|---|---|---|---|
| $(n,2n)$ | 3.9428E-03 | 3.7799E-03 | 3.9533E-03 | 4.130 | −0.267 |
| $(n,\gamma)$ | 8.1178E + 00 | 8.0229E + 00 | 8.0618E + 00 | 1.169 | 0.689 |
| $(n,removal)$ | 4.2110E + 01 | 4.2419E + 01 | 4.2458E + 01 | −0.734 | −0.827 |
| $(n,fission)$ | 3.3989E + 01 | 3.4392E + 01 | 3.3815E + 01 | −1.186 | 0.511 |

**Table 7**
Collapsed cross section comparison for U-238.

| **U-238 Cross section** | **SCALE (barn)** | **DNL (barn)** | **SSXS (barn)** | **SCALE/DNL relative difference (%)** | **SCALE/SSXS relative difference (%)** |
|---|---|---|---|---|---|
| $(n,2n)$ | 4.9885E-03 | 4.8264E-03 | 5.0008E-03 | 3.250 | −0.247 |
| $(n,\gamma)$ | 8.4397E-01 | 1.7686E + 00 | 8.4091E-01 | −109.556 | 0.363 |
| $(n,removal)$ | 9.4840E-01 | 1.8734E + 00 | 9.4516E-01 | −97.535 | 0.341 |
| $(n,fission)$ | 9.9400E-02 | 9.9219E-02 | 9.9219E-02 | 0.182 | 0.182 |

**Table 8**
Collapsed cross section comparison for Ru-103.

| Ru-103 | | | | | |
|---|---|---|---|---|---|
| **Cross section** | **SCALE (barn)** | **DNL (barn)** | **SSXS (barn)** | **SCALE/DNL relative difference (%)** | **SCALE/SSXS relative difference (%)** |
| $(n,2n)$ | 4.8411E-03 | 4.9375E-03 | 4.8530E-03 | −1.992 | −0.245 |
| $(n,\gamma)$ | 1.4487E + 00 | 5.6379E + 00 | 1.4361E + 00 | −289.172 | 0.867 |
| $(n,removal)$ | 1.4537E + 00 | 5.6431E + 00 | 1.4411E + 00 | −288.191 | 0.866 |

**Table 9**
Collapsed cross section comparison for Gd-155.

| Gd-155 | | | | | |
|---|---|---|---|---|---|
| **Cross section** | **SCALE (barn)** | **DNL (barn)** | **SSXS (barn)** | **SCALE/DNL relative difference (%)** | **SCALE/SSXS relative difference (%)** |
| $(n,2n)$ | 4.3123E-03 | 4.3951E-03 | 4.3229E-03 | −1.920 | −0.246 |
| $(n,\gamma)$ | 1.5325E + 03 | 1.5120E + 03 | 1.5270E + 03 | 1.336 | 0.358 |
| $(n,removal)$ | 1.5325E + 03 | 1.5120E + 03 | 1.5270E + 03 | 1.336 | 0.358 |

**Table 10**
U-235 collapsed cross section for 8th and 16th depletion steps.

| U-235 | | | | | | |
|---|---|---|---|---|---|---|
| | **8th depletion step** | | | **16th depletion step** | | |
| **Cross section** | **SCALE (barn)** | **SSXS (barn)** | **SCALE/SSXS relative differences (%)** | **SCALE (barn)** | **SSXS (barn)** | **SCALE/SSXS relative difference (%)** |
| $(n,2n)$ | 4.0459E-03 | 3.9859E-03 | 1.484 | 4.1296E-03 | 3.9977E-03 | 3.194 |
| $(n,\gamma)$ | 7.7398E + 00 | 7.7563E + 00 | −0.213 | 7.5850E + 00 | 7.6976E + 00 | −1.485 |
| $(n,removal)$ | 3.9436E + 01 | 3.9679E + 01 | −0.616 | 3.8299E + 01 | 3.9181E + 01 | −2.303 |
| $(n,fission)$ | 3.1692E + 01 | 3.1918E + 01 | −0.715 | 3.0710E + 01 | 3.1479E + 01 | −2.506 |

**Table 11**
U-238 collapsed cross section for 8th and 16th depletion steps.

| U-238 | | | | | | |
|---|---|---|---|---|---|---|
| | **8th depletion step** | | | **16th depletion step** | | |
| **Cross section** | **SCALE (barn)** | **SSXS (barn)** | **SCALE/SSXS relative differences** | **SCALE** | **SSXS (barn)** | **SCALE/SSXS relative difference (%)** |
| $(n,2n)$ | 4.0459E-03 | 3.9859E-03 | 1.484 | 5.2415E-03 | 5.0571E-03 | −1.376 |
| $(n,\gamma)$ | 7.7398E + 00 | 7.7563E + 00 | −0.213 | 8.3924E-01 | 8.4022E-01 | 0.445 |
| $(n,removal)$ | 3.9436E + 01 | 3.9679E + 01 | −0.616 | 9.4619E-01 | 9.4634E-01 | 0.217 |
| $(n,fission)$ | 3.1692E + 01 | 3.1918E + 01 | −0.715 | 1.0167E-01 | 1.0103E-01 | 0.639 |

**Table 12**
Ru-103 collapsed cross section for 8th and 16th depletion steps.

| Ru-103 | | | | | | |
|---|---|---|---|---|---|---|
| | **8th depletion step** | | | **16th depletion step** | | |
| **Cross section** | **SCALE (barn)** | **SSXS (barn)** | **SCALE/SSXS relative differences** | **SCALE (barn)** | **SSXS (barn)** | **SCALE/SSXS relative difference (%)** |
| $(n,2n)$ | 4.9759E-03 | 4.8930E-03 | 1.666 | 5.0870E-03 | 4.9076E-03 | 3.526 |
| $(n,\gamma)$ | 1.4708E + 00 | 1.4595E + 00 | 0.771 | 1.4821E + 00 | 1.4705E + 00 | 0.780 |
| $(n,removal)$ | 1.4759E + 00 | 1.4645E + 00 | 0.775 | 1.4873E + 00 | 1.4756E + 00 | 0.789 |

**Table 13**
Gd-155 collapsed cross section for 8th and 16th depletion steps.

| Gd-155 | | | | | | |
|---|---|---|---|---|---|---|
| | **8th depletion step** | | | **16th depletion step** | | |
| **Cross section** | **SCALE (barn)** | **SSXS (barn)** | **SCALE/SSXS relative differences** | **SCALE (barn)** | **SSXS (barn)** | **SCALE/SSXS relative difference (%)** |
| $(n,2n)$ | 4.4324E-03 | 4.3585E-03 | −1.072 | 4.5314E-03 | 4.3716E-03 | 3.527 |
| $(n,\gamma)$ | 1.3950E + 03 | 1.4144E + 03 | −1.391 | 1.3576E + 03 | 1.4091E + 03 | −3.795 |
| $(n,removal)$ | 1.3950E + 03 | 1.4144E + 03 | −1.392 | 1.3576E + 03 | 1.4091E + 03 | −3.795 |

developed coupling.

### 5.4. Fortran implementation, DTCF

In the light of previous results, the initial depletion program in Matlab® and coupling to VALKIN, DTCM, is considered validated. The final code was translated to Fortran and also coupled to VALKIN. In this implementation the solver used is *lsode*.

DTCF provided the same results as DTCM in terms of nuclide concentrations, and thus, multiplication factor. Nuclides evolutions were identical for all nuclides and depletion steps. As said previously, solving first order ODE system is a very well-known problem, most of the solvers available are suitable for solving the burnup system with acceptable results. Nevertheless, the biggest concerns in using a particular solver or

**Table 14**
Nuclide concentrations (atm/b·cm) at the end of the depletion calculation.

| Nuclide | SCALE/ORIGEN | Matlab® | Rel. Diff. (%) |
|---|---|---|---|
| Se-79 | 1.006E-07 | 1.013E-07 | −0.68 |
| Kr-83 | 1.084E-06 | 1.092E-06 | −0.72 |
| Sr-90 | 1.165E-05 | 1.174E-05 | −0.78 |
| Y-91 | 2.655E-06 | 2.699E-06 | −1.68 |
| Zr-94 | 1.377E-05 | 1.387E-05 | −0.76 |
| Mo-95 | 8.634E-06 | 8.675E-06 | −0.47 |
| Tc-99 | 1.357E-05 | 1.328E-05 | 2.16 |
| Ru-101 | 1.173E-05 | 1.181E-05 | −0.74 |
| Ag-109 | 3.931E-07 | 3.956E-07 | −0.63 |
| Sn-126 | 1.773E-07 | 1.776E-07 | −0.17 |
| I-129 | 1.431E-06 | 1.439E-06 | −0.56 |
| Xe-136 | 2.228E-05 | 2.252E-05 | −1.04 |
| Cs-133 | 1.419E-05 | 1.430E-05 | −0.76 |
| Ba-138 | 1.481E-05 | 1.493E-05 | −0.75 |
| La-139 | 1.401E-05 | 1.412E-05 | −0.75 |
| Ce-142 | 1.272E-05 | 1.281E-05 | −0.75 |
| Pr-144 | 3.284E-10 | 3.313E-10 | −0.90 |
| Nd-144 | 4.634E-06 | 4.664E-06 | −0.65 |
| Sm-147 | 4.811E-07 | 4.840E-07 | −0.61 |
| Eu-153 | 6.052E-07 | 6.072E-07 | −0.34 |
| Gd-155 | 6.369E-10 | 6.243E-10 | 1.98 |
| U-234 | 1.139E-06 | 1.141E-06 | −0.10 |
| U-235 | 8.909E-04 | 8.893E-04 | 0.18 |
| U-236 | 4.515E-05 | 4.521E-05 | −0.14 |
| U-238 | 2.169E-02 | 2.169E-02 | 0.00 |
| Np-237 | 1.542E-06 | 1.511E-06 | 1.97 |
| Pu-239 | 7.590E-05 | 7.498E-05 | 1.20 |
| Am-241 | 3.692E-08 | 3.704E-08 | −0.32 |
| Cm-244 | 3.550E-10 | 3.484E-10 | 1.85 |

method are their efficiency and computational resources consumption.

The only difference between implementations was the time required to perform the depletion calculation. On the one hand, libraries loading, and step-dependent transition matrices generation were reduced a 27 % each in DTCF, compared to DTCM. On the other hand, the main difference in the overall calculation was the time required to solve each ODE system. In general, the time required to solve the ODE systems was reduced over a 96 % by using Fortran with *lsode* solver rather than the Matlab® implementation.

In Table 15, the time required to solve the ODE systems is shown for DTCM and DTCF implementations. As it can be seen DTCF requires over 96 % less time per each depletion step. At the end, DTCM lasts over 321.24 s, whereas DTCF, with *lsode* solver, last 10.95 s to perform the whole depletion calculation, a 97 % less time.

## 6. Conclusions and future work

As one of the departing points in the development of a brand-new and modern lattice code, in the present work a general revision of available software, methods and tendencies in burnup calculations has been performed. By the end of this work the main purpose was fulfilled,

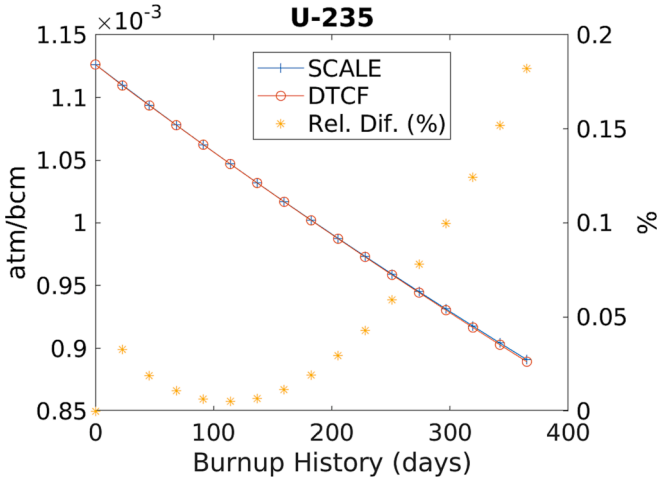


**Fig. 7.** U-235 concentration evolution.

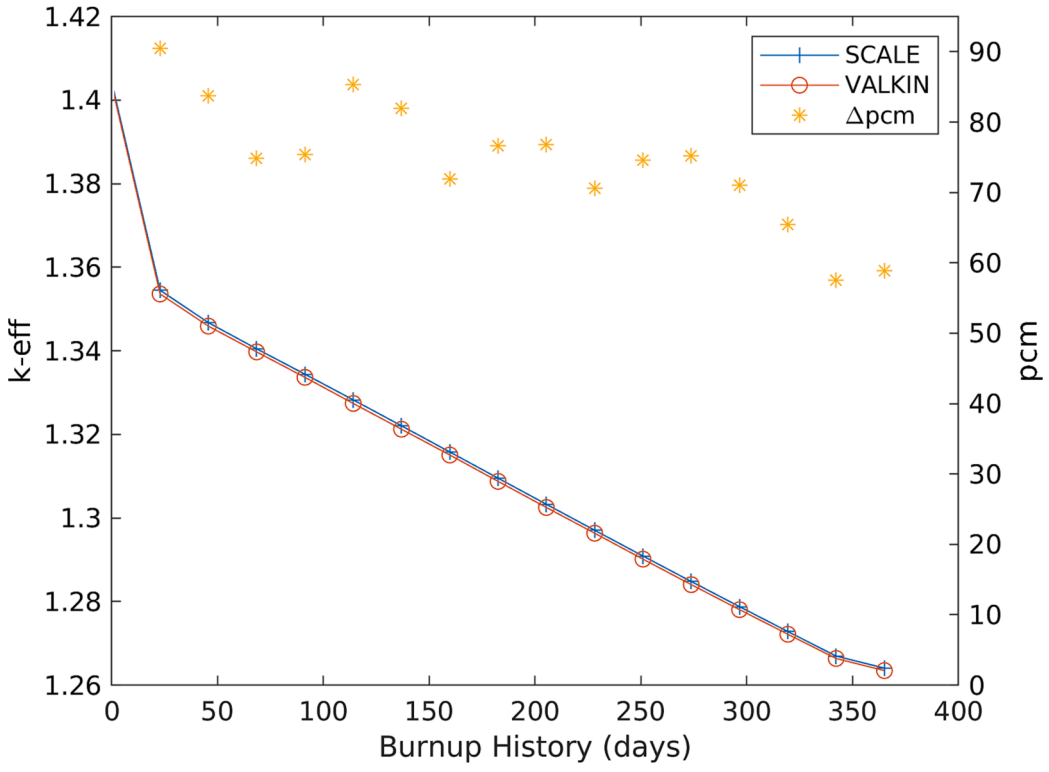


**Fig. 6.** Multiplication factor burnup evolution.

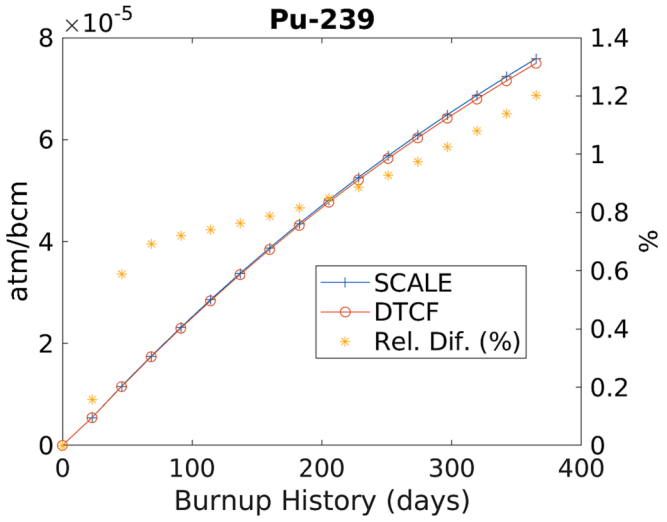


**Fig. 8.** Pu-239 concentration evolution.

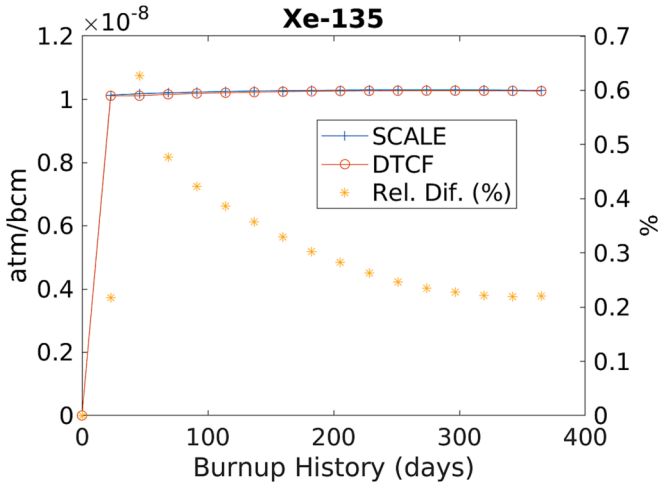


**Fig. 9.** Xe-135 concentration evolution.

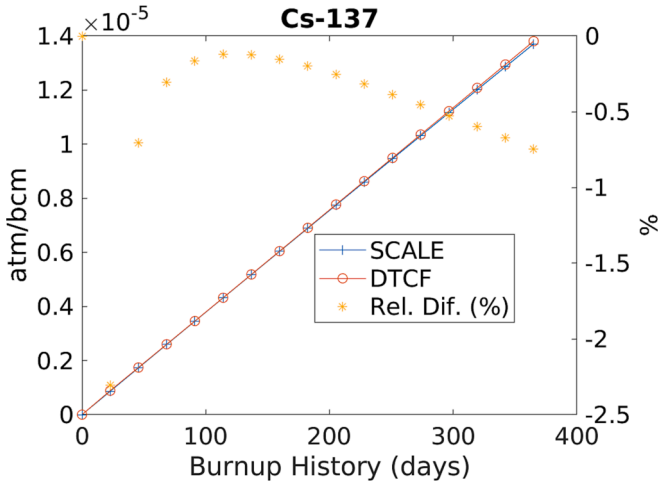


**Fig. 10.** Cs-137 concentration evolution.

data libraries, processing, and code linkage between burnup and transport programs have been studied and validated; ending up in a complete methodology to link depletion and deterministic transport codes. The burnup chain implemented is extensive, containing a great number of nuclides and possible transition, it is very detailed compared to many available codes, specially, comparing to other deterministic based burnup codes.

**Table 15**
Time reduction in ODE system solving.

| Depletion step | DTCM | DTCF | Time reduction (%) |
|---|---|---|---|
| 1 | 41.96 | 1.03 | 98 |
| 2 | 22.96 | 0.79 | 97 |
| 3 | 16.72 | 0.61 | 96 |
| 4 | 15.93 | 0.59 | 96 |
| 5 | 15.98 | 0.56 | 96 |
| 6 | 16.32 | 0.59 | 96 |
| 7 | 16.6 | 0.66 | 96 |
| 8 | 15.51 | 0.62 | 96 |
| 9 | 16.83 | 0.72 | 96 |
| 10 | 16.65 | 0.67 | 96 |
| 11 | 16.83 | 0.68 | 96 |
| 12 | 17.38 | 0.71 | 96 |
| 13 | 17.13 | 0.69 | 96 |
| 14 | 17.41 | 0.69 | 96 |
| 15 | 17.37 | 0.71 | 96 |
| 16 | 17.24 | 0.63 | 96 |

Two depletion transport codes were created and linked to VALKIN (which permits flux calculations in arbitrary unstructured meshed geometries), one implemented in Matlab® and using *ode15s*, DTCM, and one in Fortran, using *lsode*, DTCF. The resulting codes can perform depletion calculations using an extensive burnup chain. The fact that the two solvers provided the same results, in terms of concentrations evolution, proves that the nuclear data processing, accuracy, and uncertainty is the most influential matter in terms of depletion calculations. It was seen that the DTCF performance was way faster than DTCM, especially due to the use of *lsode* solver instead of *ode15s*.

VALKIN capabilities and performance have been also evaluated by obtaining good multiplication factor results for the whole depletion.

## CRediT authorship contribution statement

**Arturo Vivancos:** Investigation, Methodology, Resources, Software, Validation, Writing – original draft, Writing – review & editing. **Rafael Miró:** Conceptualization, Funding acquisition, Project administration, Supervision, Writing – original draft, Writing – review & editing. **Teresa Barrachina:** Formal analysis, Resources, Validation. **Álvaro Bernal:** Formal analysis, Resources. **Gumersindo Verdú:** Project administration, Writing – review & editing.

## Declaration of competing interest

The authors declare that they have no known competing financial interests or personal relationships that could have appeared to influence the work reported in this paper.

## Data availability

Data will be made available on request.

## Acknowledgments

This work has been partially supported by Grant PGC2018-096437-B-I00-AR funded by MCIN/AEI/ 10.13039/501100011033 and by "ERDF A way of making Europe", by the "European Union" and Grant PRE2019-089431 funded by MCIN/AEI/ 10.13039/501100011033 and by "ESF Investing in your future".

## References


Aldama, D. (2014). *International Atomic Energy Agency INDC International Nuclear Data Committee Documentation for WIMSD-formatted libraries based on ENDF/B-VII.1 evaluated nuclear data files with extended actinide burn-up chains and cross section data up to 2000 K for fuel materials*. Retrieved from http://www-nds.iaea.org/publications.

Barrachina, T., Olmo, N., Miró, R., Vivancos, A., Gallardo, S., Verdú, G., 2022. Simulation of the CROCUS REACTOR in the Framework of the H2020 CORTEX (CORE monitoring Techniques and EXperimental validation and demonstration) PROJECT. European Research Reactor Conference 329–335.

Bateman, H., 1910. Solution of a system of differential equations occurring in the theory of radioactive transformations. Proc. Cambridge Philos. Soc. 15, 423–427.

Bernal, Á. (2018). *Development of a 3D Modal Neutron Code with the Finite Volume Method for the Diffusion and Discrete Ordinates Transport Equations. Application to Nuclear Safety Analyses*.

Cacuci, D.G., 2010. 2010. Handbook of Nuclear Engineering. Boston, MA Springer, US.

Cetnar, J., 2006. General solution of Bateman equations for nuclear transmutations. Annals of Nuclear Energy 33 (7), 640–645. https://doi.org/10.1016/j.anucene.2006.02.004.

Chadwick, M.B., Obložinský, P., Herman, M., Greene, N.M., McKnight, R.D., Smith, D.L., Young, P.G., MacFarlane, R.E., Hale, G.M., Frankle, S.C., Kahler, A.C., Kawano, T., Little, R.C., Madland, D.G., Moller, P., Mosteller, R.D., Page, P.R., Talou, P., Trellue, H., van der Marck, S.C., 2006. ENDF/B-VII.0: Next Generation Evaluated Nuclear Data Library for Nuclear Science and Technology. Nuclear Data Sheets 107 (12), 2931–3060. https://doi.org/10.1016/j.nds.2006.11.001.

Chadwick, M.B., Herman, M., Obložinský, P., Dunn, M.E., Danon, Y., Kahler, A.C., Smith, D.L., Pritychenko, B., Arbanas, G., Arcilla, R., Brewer, R., Brown, D.A., Capote, R., Carlson, A.D., Cho, Y.S., Derrien, H., Guber, K., Hale, G.M., Hoblit, S., Young, P.G., 2011. ENDF/B-VII.1 nuclear data for science and technology: Cross sections, covariances, fission product yields and decay data. Nuclear Data Sheets 112 (12), 2887–2996. https://doi.org/10.1016/j.nds.2011.11.002.

DeHart, M., Zhong, Z., & Downar, T. J. (2003). TRITON: An Advanced Lattice Code for MOX Fuel Calculations. *Proc. Advances in Nuclear Fuel Management III (ANFM 2003)*.

DeHart, M. (2006). Advancements in Generalized-Geometry Discrete Ordinates Transport for Lattice Physics Calculations. *Proc. Topl. Mtg. Reactor Physics: Advances in Nuclear Analysis and Simulation (PHYSOR 2006)*. Retrieved from https://www.researchgate.net/publication/254251672.

Gauld, I. C., Radulescu, G., Ilas, G., Murphy, B. D., Williams, M. L., & Wiarda, D. (2011). Isotopic depletion and decay methods and analysis capabilities in SCALE. In Nuclear Technology (Vol. 174, Issue 2, pp. 169–195). American Nuclear Society. doi: 10.13182/NT11-3.

de Troullioud de Lanversin, J., Kütt, M., Glaser, A., 2021. ONIX: An open-source depletion code. Annals of Nuclear Energy 151. https://doi.org/10.1016/j.anucene.2020.107903.

Geuzaine, C., Remacle, J.-F., 2009. Gmsh: a three-dimensional finite element mesh generator with built-in pre-and post-processing facilities. In INTERNATIONAL JOURNAL FOR NUMERICAL METHODS IN ENGINEERING Int. J. Numer. Meth. Engng.

Haeck, W., Parsons, D. K., White, M. C., Saller, T., & Favorite, J. A. (2017). *A Comparison of Monte Carlo and Deterministic Solvers for keff and Sensitivity Calculations*.

Hernández, V., Roman, J.E., Vidal, V., 2005. SLEPc: A Scalable and Flexible Toolkit for the Solution of Eigenvalue Problems. ACM Trans. Math. Software 31 (3), 351–362.

Hindmarsh, A.C., 1983. ODEPACK, A Systematized Collection of ODE Solvers. Scientific Computing 1, 55–64.

Hu, T., Wu, H., Cao, L., Li, Z., 2017. Finite volume method based neutronics solvers for steady and transient-state analysis of nuclear reactors. Energy Procedia 127, 275–283. https://doi.org/10.1016/j.egypro.2017.08.102.

IAEA. (2007). *WIMS-D LIBRARY UPDATE*. Vienna.

Ivanov, K., Avramov, M., Kamerow, S., Kodeli, I., Satori, E., Ivanov, E., & Cabellos, O. (2013). *Benchmarks for Uncertainty Analysis in Modelling (UAM) for the Design, Operation and Safety Analysis of LWRs Volume I: Specification and Support Data for Neutronics Cases (Phase I)*. Retrieved from www.oecd-nea.org.

Josey, C., Forget, B., Smith, K., 2017. High order methods for the integration of the Bateman equations and other problems of the form of $y' = F(y, t)y$. Journal of Computational Physics 350, 296–313. https://doi.org/10.1016/j.jcp.2017.08.025.

Labarile, A., Vivancos, A., Bernal, Á., Miró, R., & Verdú, G. (2021). MULTIGROUP MATERIAL CROSS-SECTIONS GENERATION WITH SCALE 6.2.3 FOR DETERMINISTIC NEUTRON TRANSPORT CALCULATIONS. APPLICATION TO A PWR FUEL ELEMENT ANALYSIS. *M&C 2021*.

Leppänen, J., Pusa, M., Viitanen, T., Valtavirta, V., Kaltiaisenaho, T., 2015. The Serpent Monte Carlo code: Status, development and applications in 2013. Annals of Nuclear Energy 82, 142–150. https://doi.org/10.1016/j.anucene.2014.08.024.

Lindley, B.A., Hosking, J.G., Smith, P.J., Powney, D.J., Tollit, B.S., Newton, T.D., Perry, R., Ware, T.C., Smith, P.N., 2017. Current status of the reactor physics code WIMS and recent developments. Annals of Nuclear Energy 102, 148–157. https://doi.org/10.1016/j.anucene.2016.09.013.

Marguet, S. (2017). *The Physics of Nuclear Reactors*.

Marleau, G., Hébert, A., & Roy, R. (2016). *A USER GUIDE FOR DRAGON VERSION4*.

Moler, C., Van Loan, C., 2003. Nineteen dubious ways to compute the exponential of a matrix, twenty-five years later. In: SIAM Review, (Vol. 45, Issue 1,. Society for Industrial and Applied Mathematics Publications, pp. 3–49. https://doi.org/10.1137/S00361445024180.

Nea, 2005. The JEFF-3.0 Nuclear Data Library. Organisation for Economic Co-operation and Development, Paris.

Oka, Y., Madrame, H., Uesaka, M., 2014. Nuclear Reactor Design. https://doi.org/10.1007/978-4-431-54898-0.

Okumura, K., Kugo, T., Kaneko, K., Tsuchihashi, K., 2007. SRAC2006: A Comprehensive Neutronics Calculation Code. System.

Pusa, M. (2013). *Numerical methods for nuclear fuel burnup calculations*.

Radhakrishnan, K., Hindmarsh, A. C. (1993). *Description and Use of LSODE, the Livermore Solver for Ordinary Differential Equations*.

Rhodes, J., Smith, K., & Lee, D. (2006). CASMO-5 Development and Applications. *PHYSOR-2006*.

Rising, M. E., Armstrong, J. C., Bolding, S. R., Brown, F. B., Bull, J. S., Burke, T. P., Clark, A. R., Dixon, D. A., Forster III, R. A., Giron, J. F., Grieve, T. S., Hughes III, H. G., Josey, C. J., Kulesza, J. A., Martz, R. L., McCartney, A. P., McKinney, G. W., Mosher, S. W., Pearson, E. J., … Zukaitis, A. J. (2023). *MCNP® Code Version 6.3.0 Release Notes* (Issue LA-UR-22-33103, Rev.~1). Los Alamos, NM, USA. doi: 10.2172/1909545.

Romano, P.K., Horelik, N.E., Herman, B.R., Nelson, A.G., Forget, B., Smith, K., 2015. OpenMC: A state-of-the-art Monte Carlo code for research and development. Annals of Nuclear Energy 82, 90–97. https://doi.org/10.1016/j.anucene.2014.07.048.

Sanz, J., Cabellos, O., & García-Herranz, N. (2008). *ACAB software upgrade ACAB Inventory code for nuclear applications: User's Manual V. 2008*.

Schneider, D., Dolci, F., Dolci, F., Gabriel, F., Palau, J.-M., Guillo, M., Pothet, B., Archier, P., Ammar, K., Auffret, F., Baron, R., Baudron, A.-M., Bellier, P., Bourhrara, L., Buiron, L., Coste-Delclaux, M., De, C., Do, J.-M., Espinosa, B., … Zmijarevic, I. (2016). APOLLO3®: CEA/DEN Deterministic Multi-purpose code for Reactor Physics Analysis. *Proceedings of PHYSOR2016 Conf*. Retrieved from https://www.researchgate.net/publication/316684557.

Shampine, L. F., Reichelt, M. W. (1997). *THE MATLAB ODE SUITE*.

She, D., Wang, K., Yu, G., 2013. Development of the point-depletion code DEPTH. Nuclear Engineering and Design 258, 235–240. https://doi.org/10.1016/j.nucengdes.2013.01.007.

Sublet, J.C., Eastwood, J.W., Morgan, J.G., Gilbert, M.R., Fleming, M., Arter, W., 2017. FISPACT-II: An Advanced Simulation System for Activation, Transmutation and Material Modelling. Nuclear Data Sheets 139, 77–137. https://doi.org/10.1016/j.nds.2017.01.002.

Vivancos, A., Barrachina, T., Miró, R., Verdú, G., Bernal, Á., 2021. DEVELOPMENT OF A 3D DETERMINISTIC FUEL DEPLETION CODE. TopFuel.

Stankovskiy, A., Van den Eynde, G., Baeten, P., Trakas, C., Demy, P.-M., & Villate, L. (2012). ALEPH2-A general purpose Monte Carlo depletion code. *International Conference on the Physics of Reactors 2012, PHYSOR 2012: Advances in Reactor Physics. 3.*, 1861–1875. Retrieved from https://www.researchgate.net/publication/286740932.

Wagner, J. C., Peplow, D. E., Mosher, S. W., & Evans, T. M. (2011). Review of Hybrid (Deterministic/Monte Carlo) Radiation Transport Methods, Codes, and Applications at Oak Ridge National Laboratory *. In Progress in NUCLEAR SCIENCE and TECHNOLOGY (Vol. 2).

Wang, Y., Yan, L., Ma, Y., Li, W., 2017. Finite volume lattice Boltzmann scheme for neutron/radiative transfer on unstructured mesh. Annals of Nuclear Energy 109, 227–236. https://doi.org/10.1016/j.anucene.2017.05.022.

Wiarda, D., Dunn, M.E., Green, N.M., Celik, C., Petrie, L.M., 2016. AMPX-6: A Modular Code System for Processing ENDF/B. Oak Rige National Laboratory, Oak Ridge, Tenessee. Available from Radiation Safety Information Computational Center as CCC-834.

Wieselquist, W.A., Lefebvre, R.A., Jessee, M.A., 2020. SCALE Code System (6.2.4). Oak Ridge National Laboratory, Oak Ridge, TN. Retrieved from www.osti.gov.

Wemple, C. A., Gheorghiu, H-N. M., Stamm'ler C, R. J. J., Villarino, E. A. (n. d.). Recent advances in the HELIOS-2 lattice physics code. Retrieved from https://www.researchgate.net/publication/267545835.

Zhang, B., Yuan, X.B., Zhang, Y., Tang, H., Cao, L., 2020. Development of a versatile depletion code AMAC. Annals of Nuclear Energy 143. https://doi.org/10.1016/j.anucene.2020.107446.

Zhao, Z., Yang, Y., Gao, Q., 2020. Development and verification of code IMPC-Depletion for nuclide depletion calculation. Nuclear Engineering and Design 363. https://doi.org/10.1016/j.nucengdes.2020.110616.